Molecular Catalysis 476 (2019) 110520

Contents lists available at ScienceDirect

Molecular Catalysis

journal homepage: www.elsevier.com/locate/mcat

Synthesis of bio-based methacrylic acid from biomass-derived itaconic acid over barium hexa-aluminate catalyst by selective decarboxylation reaction

Ashish Bohre*, Uroš Novak, Miha Grilc, Blaž Likozar*

Department of Catalysis and Chemical Reaction Engineering, National Institute of Chemistry, Hajdrihova 19, 1000 Ljubljana, Slovenia

ARTICLE INFO

Keywords:
Biomass
Monomer
Heterogeneous catalysis
Methacrylic acid
Itaconic acid

ABSTRACT

An environmentally-benign, efficient and inexpensive high-surface-area barium hexa-aluminate ($BaAl_{12}O_{19}$, BHA) was developed as a catalyst for the decarboxylation of the biomass-derived itaconic acid (IA) to bio-based methacrylic acid (MAA). A maximal 50% final yield of MAA with a high product selectivity was obtained under relatively mild synthesis reaction conditions (250 °C; 20 bar N_2). The reported selective MAA production was elevated, operating process characteristics were significantly less harsh, and no depleting critical raw materials were utilized when paralleled to the procedures with alkaline mineral bases, noble metal-containing heterogeneous catalysis systems and unrenewable feed resources (e.g. isobutene), applied previously. It was found that the doping of palladium on BHA support (Pd@BHA) did not improve MAA productivity. The effect of the time (25–300 min), temperature (175–275 °C), pressure (10–40 bar), reacting substrate concentration (0.10–0.19 mol L^{-1}), metallic oxide mass (0.5–3.0 g) and type on IA conversion, MAA content MAA content and rates was determined, examining also recyclability. BHA catalyst was characterized with various structural techniques, such as energy-dispersive X-ray spectroscopy (EDS), X-ray powder diffraction (XRD), CO_2 temperature-programmed desorption (TPD), scanning electron microscopy (SEM) and N_2 physisorption.

Introduction

Methacrylic acid (MAA) and methyl methacrylate (MMA) are industrially important monomers, widely used in organic glass (polymethyl methacrylate), acrylic fibers, plastics, paint, and clustering agent production [1]. The current industrial manufacture of MAA and MMA is based in an acetone-cyanohydrin (ACH) process [2]. This unsustainable method relies on the use of expensive and extremely toxic feedstocks alongside corrosive concentrated acids. Besides the use of harmful substrates, low atom economy, poor product selectivity and the net emission of greenhouse gases are also drawbacks associated with the industrial process, not to mention that the production is exclusively based on a non-renewable fossil-based resource [3]. To overcome the aforementioned limitations, Mitsubishi Gas Chemicals developed an improved ACH process; however, the short catalyst lifetimes and parasitic reactions issues remain to be solved [4]. Later on, Mitsubishi Rayon developed an alternative two-step process to produce MMA via the oxidation of isobutylene to MAA and its further esterification to MMA [5].

Considering the MAA high potential, both academic and industrial researchers have attempted to derive MAA from bio-based feedstocks. In this sense, oxidative bioconversion and catalytic dehydration of biomass-derived 2-methyl-1,3-propanediol have been attempted [6]. Alternative methodology proposes the oxidative dehydrogenation of isobutyric acid (IBA) to MAA, being this prepared by lignocellulosic biomass fermentation [7]. However, the similar IBA and MAA boiling points (155 °C vs 162 °C) make this separation difficult [8,9]. In addition to the existing catalytic routes, MAA fermentative routes from renewable carbohydrates have also been envisaged using non-naturally occurring microbial organisms [10,11]. Other bio-based routes to MAA can also be accomplished using citric acid, itaconic acid, ethylene, methanol and carbon monoxide as raw materials. These can easily be obtained from biomass such as Lucite's Alpha and Evonik's AVENEER processes [12–14].

Decarboxylation is an important step, widely applied in chemical industry to obtain valuable products such as butanone, C_9-ketone, C_{17} hydrocarbon, anisol, benzyl cyanide and 2-methylbutyronitrile via the reaction of levulinic acid, 6-amyl-a-pyrone, stearic acid, ortho-anisic acid, isoleucine and phenyl alanine, respectively [15–17]. One such process involved the decarboxylation of biomass derived itaconic acid to MAA. Itaconic acid is an important platform obtained by plant biomass fermentation and can be a potential substitute for petroleum-derived chemicals such as acetone cyanohydrin, maleic acid or acrylic acid [18,19]. To the best of our knowledge, only three research articles

---

* Corresponding authors.
E-mail addresses: ashish.bohre@ki.si (A. Bohre), blaz.likozar@ki.si (B. Likozar).

https://doi.org/10.1016/j.mcat.2019.110520
Received 18 February 2019; Received in revised form 16 July 2019; Accepted 17 July 2019

Table 1

A comparison of existing routes to bio-based MAA with the present work.

Entry[a]	Catalyst	T [°C]	time	P [bar]	MAA yield [%]	Ref.
1	Pt/Al_2O_3 and NaOH	250	1 h	38	68	[20]
2	Hydrotalcite	250	15 min	34	23	[21]
3	Ruthenium carbonyl propionate	225	1.5 h	28	40	[22]
4	BHA	250	3 h	20	50	This work

[a] Reaction conditions: Reactor mode (batch), feedstock (IA), solvent (water).

have been published on catalytic decarboxylation of IA to MAA. The first report was published by Notre's group in 2014 [20], showing a good MAA yield. However, expensive Pt/Al_2O_3 catalyst and corrosive alkaline base were required to decarboxylate the IA (Table 1, entry 1). In order to avoid the use of homogenous alkali solution and expensive noble metals, Pirmoradi's group explored hydrotalcite as a solid catalyst for MAA synthesis. Unfortunately, only 23% yield of MAA was achieved (Table 1, entry 2) [21]. Recently, ruthenium carbonyl propionate complex was used as a homogenous catalyst for the decarboxylation of IA (Table 1, entry 3). Homogeneous catalysts have a general superior selectivity and specificity but their separation from the reaction is cumbersome [22]. It was reported that Pt/Al_2O_3, hydrotalcite and ruthenium carbonyl propionate complex based catalysts have a positive stabilisation effect on the itaconate monoanion and allow the decarboxylation to MAA to take place with a better selectivity. In compared to the reported catalysts the excellent catalytic activity of barium hexaaluminate is attributed to high surface area and moderate basicity that promotes the decarboxylation of IA.

Hexaaluminates are an attractive class of hexagonal aluminate materials widely used as catalysts or as a catalyst support for high temperature applications such as natural gas combustion, carbon dioxide reforming of methane, partial oxidation of hydrocarbon and nitrous oxide decomposition [23]. The high catalytic activity and remarkable thermal stability of hexaaluminates are associated with their peculiar layered structure, consisting of alternatively stacked spinel blocks of γ-Al_2O_3 and mirror planes in which large cations (La^{3+}, Ba^{2+}, Sr^{2+} etc.) are located [24]. The hexaaluminates crystal structure is dependent on the atomic radius and charge density of the large cations in the mirror planes. For instance, barium hexaaluminate (BHA) has assigned the β-Al_2O_3 structure, whereas lanthanum hexaaluminate belongs to the magnetoplumbite structure [25]. Hexaaluminate precursors are typically prepared by co-precipitation or sol-gel method. The materials crystallization at high temperature (> 1200 °C) results in low surface area 5-15 $m^2 g^{-1}$, leading to a lower amount of active sites [26]. To overcome such limitation, alternative methods have been proposed, for instances coupling of a sol–gel process in reverse microemulsions and solid-state reaction followed by two steps of ball milling. However, the aforementioned routes are hardly applicable for industrial implementation due to the high-energy-consumption, constraints of scalability, economic, and safety issues.

Inspired by the pioneer work of Santiago et al. [27], we have prepared a high surface area (96.0 $m^2 g^{-1}$) BHA catalyst through carbon templating route. The excellent catalytic activity of BHA was tested for the first time for high temperature decarboxylation reactions under subcritical water conditions. The work here described has several advantages over the previously published works [20–22]. Most notably, this work brings improvements in the use of heterogeneous catalyst by avoiding corrosive liquid base additive and precious metals like Pt and Ru. The BHA catalyst showed moderate activity and good recyclability without the doping of expensive transition metals or using homogenous catalyst (Table 1, entry 1 and entry 3).

Experimental

Preparation of catalyst

BHA catalyst was prepared through co-precipitation method. Typically, 90.03 g of $Al(NO_3)_39H_2O$ and 5.23 g of $Ba(NO_3)_2$ were dissolved in deionized water at 60 °C. Subsequently, 40 g of carbon black were added and the mixture was vigorously stirred overnight to get a slurry precursor. Likewise, 96.09 g of $(NH_4)_2CO_3$ was dissolved in 200 mL deionized water and stirred for 1 h at 60 °C. Afterwards, BHA slurry precursor was poured into an $(NH_4)_2CO_3$ solution and the mixture was vigorously stirred for 4 h to obtain a gel. The obtained gel was filtered, washed with deionized water and vacuum dried at 110 °C overnight. The resultant powder was calcined in Ar at 1250 °C for 5 h, followed by calcination at 900 °C in air for 12 h to completely remove the carbon, leading to a high surface area BHA catalyst.

Pd/BHA catalyst was prepared by a deposition–precipitation (DP) procedure. In a typical procedure, 1 g of BHA support was added to 20 mL aqueous solution containing 250 mg of $Pd(NO_3)_2$. The pH of the solution was adjusted to 9 by adding 0.2 M NH_4OH under vigorous stirring. The mixture was then stirred for 1 h at 60 °C. After cooling to room temperature, the solid was recovered by filtration and washed with distilled water. The mixture was then placed in a vacuum oven and allowed to dry overnight at 40 °C. The dried material was then transferred to a Schwartz-type drying tube and reduced in a H_2 flow at 350 °C for 3 h. The Pd/BHA catalyst was subsequently cooled to room temperature under flowing N_2. g-C_3N_4 catalyst was prepared from urea precursor by adopting the reported method [40].

The as-synthesized BHA catalyst was characterized by Powder X-ray diffraction, Temperature programmed desorption, scanning electron microscope (SEM) and transmission electron microscope (TEM). The detailed information is available in supporting information.

Catalytic decarboxylation

Decarboxylation reactions were performed in a high pressure batch reactor (250 mL, Amar Equipment Pvt. Ltd., India) equipped with a thermocouple, pressure gauge, rupture disk, gas and liquid sampling line. In a typical experiment, 2 g of itaconic acid was dissolved in 150 mL of deionized water. The solution was loaded into the autoclave reactor with a catalyst (1 g) and sealed. The reactor was pressurized with N_2 to 10 bar and vented three times to remove any residual oxygen. Finally, the reactor was pressurized to 20 bars with N_2, stirred by the Rushton turbine (600 min^{-1}) and heated up to 250 °C. It had been previously determined that under the stirring speed of 600 min^{-1} the reaction was conducted in the kinetic regime, since using higher stirring rates did not increase the conversion. Most of the experiments were performed under kinetic regime. We have taken the samples with respect to time as seen in the Fig. S1. However the selectivity of MAA has not improved at low IA conversion.The final temperature was reached in 45 min and the autogenic pressure reached 52 bar, which remained constant during the experiment. The recorded reaction time started when the temperature reached the desired set-point. Once the reaction was completed, the reactor was cooled-down to the room temperature (20 °C). After collecting the final gas and liquid sample, pressure from the headspace of the reactor was released. The crude reaction mixture was analysed by UHPLC (liquid phase) and micro-GC (gas phase).

MAA extraction and purification procedure

After reaction has occurred, the catalyst was separated by centrifugation and the resultant liquid was collected in a round bottom flask. The residual MAA in the aqueous solution was extracted by Et_2O (3 × 50 mL), and the combined organic layers were dried over $MgSO_4$ while Et_2O was removed *in vacuo*. Lastly, the purified MAA was obtained after the vacuum distillation (20 mbar) at 40 °C for more than

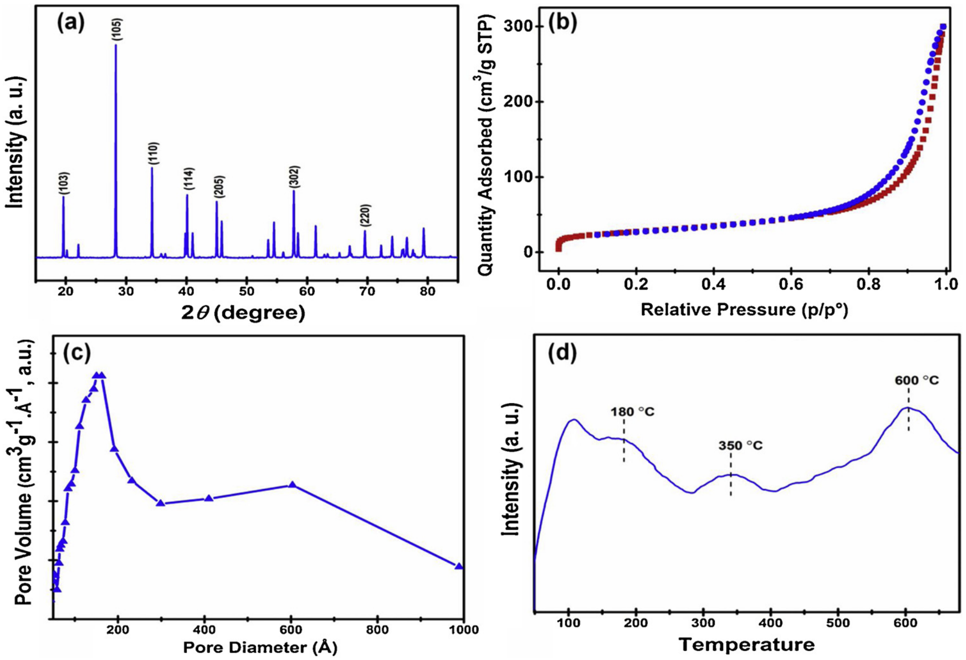

Fig. 1. (a) XRD pattern, (b) Nitrogen adsorption-desorption isotherm, (c) pore size distribution, and (d) CO_2-TPD profile of the BHA catalyst.

2 h. The isolated MAA was analyzed by NMR spectroscopy. Both ^1H and ^{13}C NMR spectra of the liquid product revealed the isolation of a pure MAA (Fig. S2-S3).

MAA: ^1H NMR ($CDCl_3$, 400 MHz): $\delta = 1.98$ (dd, 3 H), 5.71 (m, 1 H), 6.28 (m. 1 H), 11.60 ppm (br s, 1 H); ^{13}C NMR ($CDCl_3$): $\delta = 17.84$, 127.87, 135.75, 173.19 ppm.

Results and discussion

Structural and physicochemical characterization

The powder XRD pattern of BHA catalyst (Fig. 1a) showed diffraction peaks at 19.6°, 28.3°, 343° 40.1°, 45.1°, 57.7°, and 69.6° corresponding to the (103), (105), (110), (114), (205), (302), and (220) planes of BHA (JCPDS card, file no. 00-026-0135, $BaAl_{12}O_{19}$ phase), respectively [28]. The strong and sharp diffraction peaks indicate that a relatively pure BHA crystalline phase was obtained after calcination at 1250 °C. In the XRD pattern of Pd/BHA catalyst (Fig. S4) the Pd peaks at 40.1°, 46.6°, and 68.1 were attributed to the (111), (200), and (220) planes of the face centered cubic structure of Pd (JCPDS card, file no. 46–1043), respectively. The X-ray diffraction pattern of g-C_3N_4 (Fig. S5) displays one strong diffraction peak at 27.4° corresponds to (0 0 2) plane which depicts the interlayer stacking of conjugated aromatic systems of graphene related materials (g-C_3N_4) which is in consistent with the literature (JCPDS card, file no. 87-1526).

The nitrogen adsorption-desorption isotherms and BJH (Barrett-Joyner-Halenda) pore size distribution curves of BHA catalyst are shown in Fig. 1b–c. It can be observed that the catalyst demonstrated type-IV curve with hysteresis loop lying at a relative pressure (p/p°) of 0.70-0.89, indicating the presence of uniform cylindrical mesoporous channels [29], On the other hand, the BJH pore size distribution curve of BHA catalyst exhibits pore size distribution in the macroporous and mesoporous regions. It was also observed that BHA catalyst possessed a high BET specific surface area and a pore volume of 96.0 $m^2\,g^{-1}$ and 0.46 $cm^3\,g^{-1}$, respectively. These are a result of the carbon black addition as a hard templating agent, which prevents the particles agglomeration during the high temperature calcination process [30].

Since basicity plays a crucial role in the decarboxylation reactions, the basicity strength of the prepared BHA catalyst was determined by the temperature programmed desorption of CO_2. Results showed four desorption peaks with different basic strength distributed on the surface of BHA catalyst (Fig. 1d). The profile of BHA catalyst exhibited a large amount of desorbed CO_2 at 350 °C, implying the presence of low and medium basic sites. These could be associated with the surface of HO^- and Al^{3+}-O^{2-} Lewis acid-base pairs. The desorption peak at 600 °C; can be ascribed to the strong base site type related to a low-coordination surface of O^{2-} anion [31]. The total amount of basic sites in BHA catalyst was 3.05 $\mu mol\,g^{-1}$. The SEM image of BHA catalyst is shown in Fig. 2a, where it can be seen irregular aggregates. Regarding the BHA catalyst TEM images (Fig. 2 b–d), two distinctive morphologies can be clearly seen, namely one with big crystallites and the other with small agglomerates. The big crystallites seem to grow in the form and shape of platelets. Small agglomerates show features in the form of needles or 3D worm-like. Selected area electron diffraction (SAED) pattern demonstrated the monocrystalline characteristic of the catalyst (Fig. 2c, inset). According to the EDX maps, Ba is well incorporated into the big crystallites (Fig. S6).

Selective decarboxylation of itaconic acid

In order to determine the influence of the reaction temperature on the BHA catalyst performance, the experiments were conducted in the temperature range of 175–275 °C (Table 2, entry 1–5). At low temperatures (175–200 °C), the IA conversion is incomplete and the selectivity towards MAA is low. Nevertheless, upon increasing the reaction temperature from 200 to 250 °C, the MAA selectivity was increased from 19 to 30% with a complete IA conversion. By further increasing the reaction temperature to 275 °C, the MAA selectivity decreased once again to 27%. This might be due to the side reactions (dehydration and decarboxylation) that take place at high temperature (Scheme 1) [32].

The catalytic activity was further investigated by tuning the reaction pressure in the second set of experiments, while temperature was kept constant at the previous optimized value (Table 2, Entry 6–8). As expected, the catalytic reaction performed at low pressure led to a poor MAA selectivity. Yet, when the reaction was performed at 20 bar N_2 pressure, the decarboxylation rate increased and reached a MAA selectivity maximum of 50%. Furthermore, when the pressure was increased ($>$ 30 bar) under these conditions, the MAA selectivity

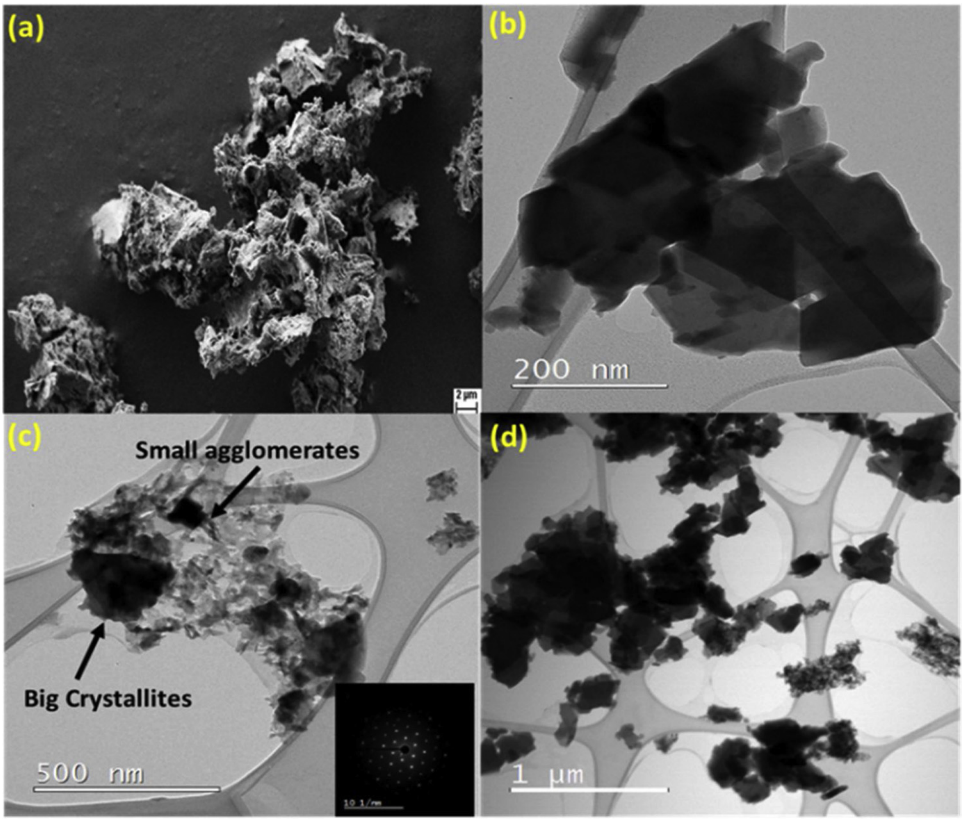

Fig. 2. (a) SEM image, (b–d) TEM images, and SAED pattern (inset) of the BHA catalyst.

decreased and the formation of side products predominated, indicating that a higher pressure is not favorable in this case. Notably, under these reaction conditions, a 4 bar increase of the internal pressure was observed probably caused by the formation of gaseous by-product (propene) due to the subsequent decarboxylation step (Scheme 1, Fig. S7) [33]. Our initial experiment that used a 0.15 M itaconic acid resulted in complete conversion after 3 h at 250 °C (Table 2, entry 7). The MAA selectivity reached 50%, and the rest of the products consisted of degradation products. If we decreased the substrate concentration to 0.10 M, the level of MAA selectivity decreased slightly to 45% (Table 2, entry 9). If we increased the substrate concentration to 0.20 M, a lower MAA selectivity (32%) was obtained and yield of degradation products increased to 45% (Table 2, entry 10).

In the third set of experiments, we have varied reaction time, and catalyst dosages. Unfortunately, it did not improve the MAA selectivity (Table 2, entry 11–14). The screening experiments suggested that a

Table 2
Screening of reaction conditions for decarboxylation of itaconic acid with BHA catalyst.

Entry[a]	*T* [°C]	*P* [bar]	Conversion [%]	Selectivity [mol %]				
				MAA	Isomers[b]	2-HIBA	AA	Others[c]
1	175	40	80	15	31	–	19	35
2	200	40	87	19	23	6	20	32
3	225	40	92	25	6	9	23	37
4	250	40	100	30	2	11	14	43
5	275	40	100	27	–	5	12	56
6	250	10	100	24	3	8	21	44
7	250	20	100	50	–	18	3	29
8	250	30	100	45	–	19	2	33
9[d]	250	20	100	45	–	18	1	36
10[e]	250	20	100	32	–	22	1	45
11[f]	250	20	100	44	–	20	1	35
12[g]	250	20	100	42	–	23	1	34
13[h]	250	20	100	47	–	23	5	25
14[i]	250	20	100	49	–	23	4	24

[d–e] IA = 0.10 M & 0.20 M.

[f–g] Catalyst = 2 g & 3 g.

[h–i] Time (4 h & 5 h). Values were determined by HPLC and micro-GC. IA is itaconic acid, MAA is methacrylic acid, AA is acetic acid and 2-HIBA is 2-hydroxyisobutyric acid.

[a] Reaction conditions : IA = 0.15 M, solvent (water), time (3 h), BHA catalyst = 1 g.

[b] isomers = mesaconic acid + citraconic acid.

[c] Others = pyruvic acid, crotonic acid, acetone, propene and carbon dioxide.

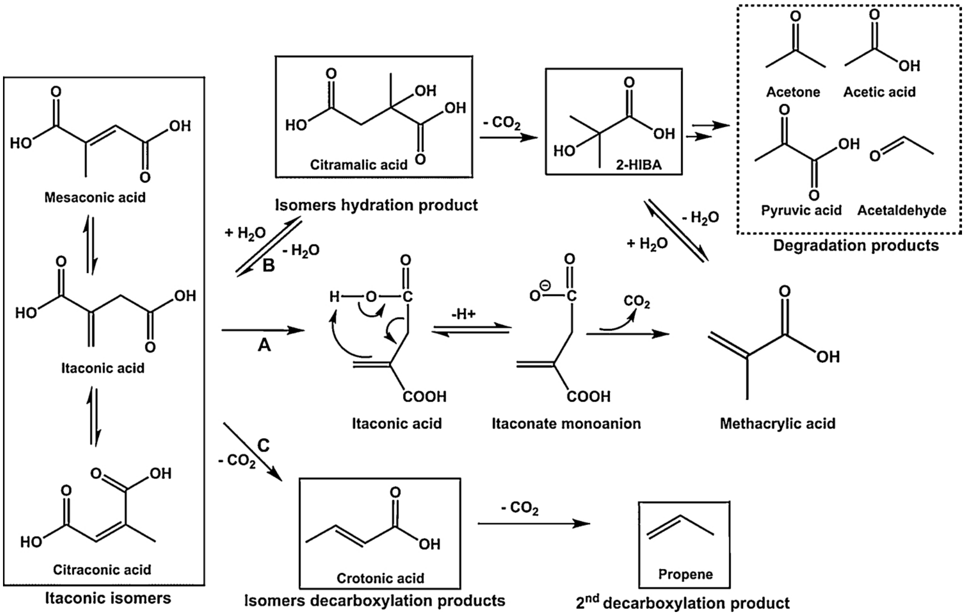

Scheme 1. Proposed catalytic mechanistic pathways to form methacrylic acid and by-products on BHA catalyst.

reaction temperature of 250 °C, 20 bar pressure, 1 g of BHA catalyst and reaction time of 3 h offered the highest MAA yield (50%) and low by-product formation within the tested window of process parameters.

With the optimized decarboxylation reaction conditions in hand, the next investigation was conducted on a series of as-prepared catalysts (Table 3). For the initial proof of concept, we have started our experiment with a homogenous NaOH catalyst. It was found that the conversion of IA was high but the selectivity towards the MAA was low (Table 3, entry 1). This agrees with the literature data that shows that the higher concentration of OH^- in the reaction mixture quenches the decarboxylation reaction, leading to a lower yield of the desired product [32]. It has also been reported in literature that the addition of NaOH as a co-catalyst is able to improve the decarboxylation product yield by suppressing the hydration of double bonds [34].

However, in case of BHA catalyst, the NaOH addition impairs the catalytic activity (Table 3, entry 2), presumably due to the adsorption of by-products on the surface of BHA catalyst that could block the active sites [35]. Afterwards, we tested the catalytic activity of graphitic carbon nitride (g-C_3N_4) for the decarboxylation of MAA. g-C_3N_4 catalyst was of great interest owing to its Lewis-base character, layered structure and number of surface defects, which can be useful in the decarboxylation reaction [36,37]. Unfortunately, g-C_3N_4 catalyst gets solubilized during the reaction under our reaction conditions resulting in a low MAA yield (Table 3, entry 3, Fig. S8).

There are some reports that Pd containing materials are robust catalyst for the decarboxylation of itaconic acid reactions [20,34]. In light on these studies, we have designed Pd catalyst supported on BHA for the itaconic acid decarboxylation. It was observed that the addition of Pd metal (10 wt %) in the BHA catalyst matrix did not improve the MAA yield (Table 3, entry 7) probably due to the low surface area of Pd/BHA catalyst (Fig. S9). It is believed that the high BHA catalytic activity compared to the other tested catalysts is associated with its moderate basicity and high surface area [38,39]. Moreover, the large cations (Ba^{2+}, Ca^{2+}, Sr^{2+}) stabilized in the matrix of hexaaluminates are able to maintain a relative activity and superior stability under subcritical water conditions [31]. These large cations provide the appropriate basic capacity that could also improve the catalytic activity of BHA. It was evident from the solvent variation experiment that water is a necessary component in our reaction medium, as it mitigates the formation of anhydrides as evident by the solvent variation experiments (Table S2) [23].

To demonstrate the recyclability of the BHA catalyst, the reaction was carried out in four consecutive repetitive cycles. As shown in Fig. 3, the MAA yield decreased from 50% (1st cycle) to 37% (4th cycle). This could also be partly attributed to the loss of the catalyst mass (7%) during the recovery, which can also accounts for the variation in catalytic activity. The XRD and CO_2-TPD analysis of the used BHA catalyst confirmed that the reaction conditions have not induced the structural and textural modifications (Fig. S10-S11).

Reaction mechanism

The proposed catalytic mechanistic pathways relating to formation of MAA and other by-products are provided in Scheme 1. The formation of MAA is that IA firstly isomerized to mesaconic acid and citraconic acid mainly over the weak acid sites on the catalyst. In the second step abstraction of proton from IA was occurred on the surface of the BHA catalyst.

The carbonium ion generated during this process was decarboxylates to MAA by leaving the β-carboxyl group. The second decarboxylation of MAA produced propene that we have identified in the gas phase analysis (Fig. S7, Scheme 1, reaction A). We have not detected 2-hydroxyisobutyric acid in the reaction mixture that confirmed that the hydration of MAA is not possible during the reaction. Interestingly, the formation of by-products was started from the beginning by following parallel pathways.

Under hydrothermal conditions in reaction B, citramalic acid was produced by the hydration of any of the three itaconic acid isomers. However, we have not detected the citramalic acid in our reaction

Table 3
Comparison of the activity of BHA with different catalysts.

Entry[a]	Catalyst	Conversion [%]	Yield of MAA (%)
1	NaOH[b]	87	10
2	BHA/NaOH	95	32
3	g-C_3N_4	79	20
4	Pd/BHA	100	46
5	BHA	100	50

[a] Reaction conditions : IA = 0.15 M, solvent (water), time (3 h), temperature 250 °C, pressure 20 bar, catalyst = 1 g.

[b] NaOH = 2 equivalents.

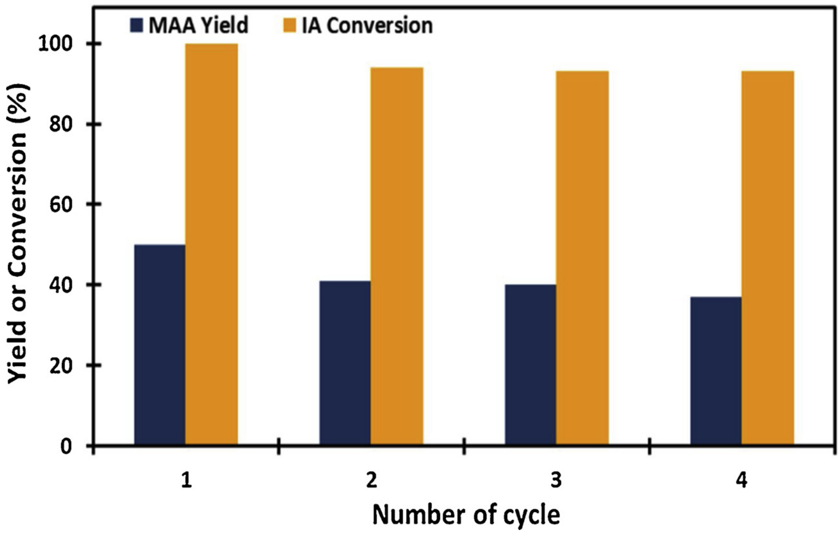

Fig. 3. Recyclability of the BHA catalyst. Reaction conditions: Itaconic acid (2 g), water (150 mL), catalyst (1 g), initial pressure (20 bar).

mixture. Citramalic acid is not stable and further decarboxylate to 2-hydroxyisobutyric acid (2-HIBA) that subsequently produced different degradation products such as pyruvic acid, acetic acid, acetone and acetaldehyde. Propene can also be produced by following pathway C.

Conclusion

We have developed a new system for the highly selective decarboxylation of IA to MAA using BHA catalyst. A number of important parameters have been studied, and it was found that the reaction temperature and pressure had a considerable effect on IA conversion and MAA selectivity. Under optimal conditions, a complete conversion of IA and a MAA yield of 50% were obtained after 3 h at 250 °C. Our catalytic system has demonstrated two important advantages: (a) it did not require a homogeneous alkaline base or loading of expensive noble metals and (b) the catalyst shows high catalytic activity under relatively mild reaction conditions.

Extensive solid-state characterization using spectroscopic techniques revealed that a high BHA catalytic activity associated with its moderate basicity and high surface area. To the best of our knowledge, this is the first report of this method on the selective and high yield production of MAA from biomass-derived itaconic acid over a heterogeneous catalyst under mild reaction conditions in absence of corrosive mineral base. The current systems leave room for optimization, and especially the decarboxylation of biomass-derived substrates to MAA at low temperature is one of the most appealing starting-points to commercialize this process. We are currently developing this chemistry further through catalyst and process design with specific application towards scale-up.

Acknowledgements

The authors gratefully acknowledge the financial support of the Slovenian Research Agency (ARRS) through the Program P2-0152. The work was partially carried out within the RDI project Cel. Cycle: Potential of biomass for the development of advanced materials and bio-based products», co-financed by the Republic of Slovenia, Ministry of Education, Science and Sport and European Union under the European Regional Development Fund, 2016-2020.

Appendix A. Supplementary data

Supplementary material related to this article can be found, in the online version, at doi:https://doi.org/10.1016/j.mcat.2019.110520.

References

[1] M.J.D. Mahboub, J.L. Dubois, F. Cavani, M. Rostamizadeh, G.S. Patience, Catalysis for the synthesis of methacrylic acid and methyl methacrylate, Chem. Soc. Rev. 47 (2018) 7703–7738.
[2] K. Nagai, New developments in the production of methyl methacrylate, Appl. Catal. A 221 (2001) 367–377.
[3] Y. Hu, G. Jiang, G. Xu, X. Mu, Hydrogenolysis of lignin model compounds into aromatics with bimetallic Ru-Ni supported onto nitrogen-doped activated carbon catalyst, Mol. Catal. 445 (2018) 316–326.
[4] Y.L. Cao, L. Wang, L.L. Zhou, B.H. Xu, Y.Y. Diao, S.J. Zhang, A modified heteropoly acid catalyst with cetyltrimethylammonium bromide for methacrolein to methacrylic acid, J. Ind. Eng. Chem. 65 (2018) 254–263.
[5] L. Zhou, L. Wang, S. Zhang, R. Yan, Y. Diao, Effect of vanadyl species in Keggin-type heteropoly catalysts in selective oxidation of methacrolein to methacrylic acid, J. Catal. 329 (2015) 431–440.
[6] S.H. Pyo, T. Dishisha, S. Dayankac, J. Gerelsaikhan, S. Lundmark, N. Rehnberg, R. Hatti-Kaul, A new route for the synthesis of methacrylic acid from 2-methyl-1, 3-propanediol by integrating biotransformation and catalytic dehydration, Green Chem. 14 (2012) 1942–1948.
[7] K. Zhang, A.P. Woodruff, M. Xiong, J. Zhou, Y.K. Dhande, A synthetic metabolic pathway for production of the platform chemical isobutyric acid, ChemSusChem 4 (2011) 1068–1070.
[8] A. Morschbacker, Bio-ethanol based ethylene, J. Macromol. Sci. Polymer Rev. 49 (2009) 79–84.
[9] B.N.M. van Leeuwen, A.M. van der Wulp, I. Duijnstee, A.J.A. van Maris, A.J.J. Straathof, Fermentative production of isobutene, Appl. Microbiol. Biotechnol. 93 (2012) 1377–1387.
[10] T. Nagasawa, T. Nakamura, H. Yamada, Production of acrylic acid and methacrylic acid using Rhodococcus rhodochrous J1 nitrilase, Appl. Microbiol. Biotechnol. 34 (3) (1990) 322–324.
[11] A.P. Burgard, M.J. Burk, R.E. Osterhout, P. Pharkya, Microorganisms for the production of methacrylic acid, US8241877, 2012.
[12] S. Ziemian, I.A. York, A Process for the Production of Ethylenically Unsaturated Carboxylic Acids or Esters and a Catalyst Therefor, EP1176366A2 (2005).
[13] L. Zhoua, L. Wanga, Y. Diao, R. Yana, S. Zhang, Cesium salts supported heteropoly acid for oxidation of methacrolein to methacrylic acid, Mol. Catal. 433 (2017) 153–161.
[14] L. Zhoua, L. Wang, Yunli Cao, Y. Diao, R. Yan, S. Zhang, The states and effects of copper in Keggin-type heteropolyoxometalate catalysts on oxidation of methacrolein to methacrylic acid, Mol.Catal. 438 (2017) 47–54.
[15] P. Tuhin, D. Maiti, Decarboxylation as the key step in C-C bond-forming, Chem. Eur. J. 23 (2017) 7382–7401.
[16] M.I. Alam, S. Gupta, A. Bohre, E. Ahmad, T.S. Khan, B. Saha, M.A. Haider, Development of 6-amyl-α-pyrone as a potential biomass-derived platform molecule, Green Chem. 18 (2016) 6431–6435.
[17] A.V. Ignatchenko, J.P. McSally, M.D. Bishop, J. Zweigle, Ab initio study of the mechanism of carboxylic acids cross-ketonization on monoclinic zirconia via condensation to beta-keto acids followed by decarboxylation, Mol. Catal. 441 (2017) 35–62.
[18] J.L. Ramos, Z. Udaondo, B. Fernández, C. Molina, A. Daddaoua, A. Segura, E. Duque, First-and second-generation biochemicals from sugars: biosynthesis of itaconic acid, Microb. Biotechnol. 9 (2016) 8–10.
[19] S.T. Ahmed, N.G.H. Leferink, N.S. Scrutton, Chemo-enzymatic routes towards the synthesis of bio-based monomers and polymers, Mol. Catal. 467 (2019) 95–110.
[20] J.L. Nôtre, S.W. Dijk, J.V. Haveren, E.L. Scott, J.P. Sanders, Synthesis of bio-based methacrylic acid by decarboxylation of itaconic acid and citric acid catalysed by

solid transition-metal catalysts, ChemSusChem 7 (2014) 2712–2720.
[21] M. Pirmoradi, J.R. Kastner, Synthesis of methacrylic acid by catalytic decarboxylation and dehydration of carboxylic acids using a solid base and subcritical water, ACS sustain. Chem. Eng. 5 (2016) 1517–1527.
[22] J.C. Lansing, R.E. Murray, B.R. Moser, Biobased methacrylic acid via selective catalytic decarboxylation of itaconic acid, ACS Sustain. Chem. Eng. 5 (2017) 3132–3140.
[23] N. Iyi, S. Takekawa, S. Kimura, Crystal chemistry of hexaaluminates: β-alumina and magnetoplumbite structures, J. Solid State Chem. 83 (1989) 8–19.
[24] Y. Zhang, X. Wang, Y. Zhu, X. Liu, T. Zhang, Thermal evolution crystal structure and Fe crystallographic sites in $LaFe_xAl_{12-x}O_{19}$ hexaaluminates, J. Phys. Chem. A 118 (2014) 10792–10804.
[25] G. Groppi, M. Bellotto, C. Cristiani, P. Forzatti, P. Villa, Thermal evolution crystal structure and cation valence of Mn in substituted Ba-β-Al_2O_3 prepared via coprecipitation in aqueous medium, J. Mater. Sci. 34 (1999) 2609–2620.
[26] P. Forzatti, L. Lietti, Catalyst deactivation, Catal. Today 52 (1999) 165–181.
[27] M. Santiago, J.C. Groen, J. Pérez-Ramírez, Carbon-templated hexaaluminates with enhanced surface area and catalytic performance, J. Catal. 257 (2008) 152–162.
[28] L. Liotta, G. Deganello, D. Sannino, M. Gaudino, P. Ciambelli, S. Gialanella, Influence of barium and cerium oxides on alumina supported Pd catalysts for hydrocarbon combustion, Appl. Catal. A 229 (2002) 217–227.
[29] M. Manikandana, M. Prabu, S.K.A. Kumar, P. Sangeetha, R. Vijayaraghavan, Tuning the basicity of Cu-based mixed oxide catalysts towards the efficient conversion of glycerol to glycerol carbonate, Mol. Catal. 460 (2018) 53–62.
[30] S. Pyena, E. Honga, Mi Shin, Y.-W. Suh, C.-H. Shin, Acidity of co-precipitated SiO_2-ZrO_2 mixed oxides in the acid-catalyzed dehydrations of iso-propanol and formic acid, Mol. Catal. 448 (2018) 71–77.
[31] M. Tian, X. Wang, T. Zhang, Hexaaluminates: a review of the structure, synthesis and catalytic performance, Catal. Sci. Technol. 6 (2016) 1984–2004.
[32] M. Carlsson, C. Habenicht, L.C. Kam, M.J.J. Antal, N. Bian, R.J. Cunningham, M.J. Jones, Study of the sequential conversion of citric to itaconic to methacrylic acid in near-critical and supercritical water, Ind. Eng. Chem. Res. 33 (1994) 1989–1996.
[33] A. Bohre, B. Hočevar, M. Grilc, B. Likozar, Selective catalytic decarboxylation of biomass-derived carboxylic acids to bio-based methacrylic acid over hexaaluminate catalysts, Appl. Catal. B Environ. 256 (2019) 117889.
[34] J. Verduyckt, D.E. De Vos, Highly selective one-step dehydration, decarboxylation and hydrogenation of citric acid to methylsuccinic acid, Chem. Sci. 8 (2017) 2616–2620.
[35] E.M. Johansson, K.J. Danielsson, E. Pocoroba, E.D. Haralson, S.G. Jaras, Catalytic combustion of gasified biomass over hexaaluminate catalysts: influence of palladium loading and ageing, Appl. Catal. A 182 (1999) 199–208.
[36] J. Zhu, P. Xiao, H. Li, S.A. Carabineiro, Graphitic carbon nitride: synthesis, properties, and applications in catalysis, ACS Appl. Mater. Interfaces 6 (2014) 16449–16465.
[37] N.S. Kus, Organic reactions in subcritical and supercritical water, Tetrahedron 4 (2012) 949–958.
[38] J.G. Park, A. Cormack, Crystal/Defect structures and phase stability in Ba hexaaluminates, J. Solid State Chem. 121 (1996) 278–290.
[39] S.Q. Wang, Z.W. Wang, L.C. Yang, Jl. Dong, C.Q. Chi, D.N. Sui, Y.Z. Wang, J.G. Ren, M.Y. Hung, Y.Y. Jiang, A novel efficient route for preparation of chiral β-hydroxycarboxylic acid: asymmetric hydration of unsaturated carboxylic acids catalyzed by heterobimetallic complex wool–palladium–cobalt, J. Mol. Catal. 264 (2007) 60–65.
[40] S. Martha, A. Nashim, K. Pardia, Facile synthesis of highly active g-C_3N_4 for effecent hydrogen production under visible light, J. Mater. Chem. A 1 (2013) 7816–7824.